



23rd IAHR International Symposium on Ice
Ann Arbor, Michigan, USA, May 31 to June 3, 2016

Multi-Sensor Approach to Ice Type Classification, Ice Thickness Measurement, and Ice PAR Attenuation in the Great Lakes

LESHKEVICH, G.¹, NGHIEM, S.V.², HALL, D.K.³, and SHUCHMAN, R.⁴

¹*NOAA/Great Lakes Environmental Research Laboratory
4840 South State Road, Ann Arbor, Michigan 48108
george.leshkevich@noaa.gov*

²*Jet Propulsion Laboratory, California Institute of Technology
4800 Oak Grove Drive, MS 300-235, Pasadena, California 91109
son.v.nghiem@jpl.nasa.gov*

³*Earth Systems Science Interdisciplinary Center (ESSIC)
University of Maryland, College Park, MD 20742
dkhall1@umd.edu*

⁴*Michigan Tech Research Institute
3600 Green Court, Suite 100, Ann Arbor, MI 48105
shuchman@mtu.edu*

Abstract

Measurements of ice type, concentration, thickness, and transmittance are essential for modeling ice growth, wintertime primary productivity estimates, as well as for Coast Guard ice breaking operations in the Great Lakes. This paper describes the use of optical, synthetic aperture radar (SAR), and scatterometer sensors to retrieve those measurements from satellite and airborne platforms. Initial validation of a satellite SAR algorithm to classify Great Lakes ice types showed that ice types can be classified using a library of ice backscatter signatures, but that open water can be misclassified owing to the ambiguity in single polarization data due to variations in wind speed/direction over water. RADARSAT-2 Quad-pol data was used to first create an ice/water mask for both small and large incidence angle SAR data. However, distinguishing ice and water is problematic using RADARSAT-2 ScanSAR Wide data owing to the wide range of incident angles in the data. Using Moderate-Resolution Imaging Spectroradiometer (MODIS) thermal infrared data to distinguish ice and water by surface temperature can remediate the ambiguity, after which the backscatter library can be used to classify ice types. Ice and water can also be identified using dual polarized scatterometer data as well as ice freeze-up and break-up dates. Over open water in Lake Superior, RADARSAT-2 SAR revealed features corresponding to cloud streets in MODIS observations. To aid in estimating lake-wide photosynthetically active radiation (PAR) transmittance through ice, in situ measurements of PAR (400-700 nm) transmittance through major ice types can be used with the maps of ice type to estimate lake-wide transmittance. Until satellite algorithms are developed for ice thickness retrieval, an airborne ground penetrating radar (GPR) can acquire ice thickness transects more effectively than in situ measurement methods. Test flights of a GPR on a helicopter over snow

ice/lake ice were made producing acceptably accurate ice thickness. Autonomous drones, tested in March 2016 for real-time ice reconnaissance, may serve as a platform for GPR measurements.

1. Satellite SAR Ice Type Classification

In the Great Lakes, the world's largest freshwater surface covering an area of 245,000 km² with a drainage basin extending 1,110 km north-south and 1,390 km east-west, ice cover is inherently a large-scale problem. The ice cover of the Great Lakes is a strong climate indicator, and its seasonal change in surface cover has a profound impact on regional environment, ecology, economics, navigation, and public safety. Great Lakes ice cover information, including spatial coverage, concentration, ice type, thickness, freezeup and breakup dates, and ice duration, is an important and necessary input for environmental protection and management, ice breaking operations, and ice forecasting and modeling efforts. Owing to the size and extent of the Great Lakes and the variety of ice types found there during the winter, the timely and objective qualities in computer processing of satellite data make it well suited for such studies.

Recommendations for Great Lakes ice research made by Marshall (1966), conclude that “studies are needed to classify Great Lakes ice types, their distribution and drift during the winter, and the subtle changes in albedo and imagery which mark the gradual disintegration of the ice and the imminent breakup.” which still apply. Early investigations by various researchers were conducted to classify and categorize ice types and features (Chase 1972, Bryan 1975), to map ice distribution (McMillan and Forsyth 1976, Leshkevich 1976), and to monitor and attempt to forecast ice movement with remotely sensed data (Strong 1973, McGinnis and Schneider 1978, Rumer *et al.* 1979, Schneider *et al.* 1981). Most of the early classification and mapping research on Great Lakes ice cover was done by visual interpretation of satellite and other remotely sensed data (Rondy 1971, Schertler *et al.* 1975, Wartha 1977). The extensive nature of ice cover in the Great Lakes and in connecting channels demands the use of satellite SAR data to satisfy the required high spatial resolution and the large aerial coverage simultaneously. The all-weather, day-and-night sensing capabilities of SAR make it well suited to monitoring winter conditions in the Great Lakes, provided that data analysis algorithms can be developed.

During the 1997 winter season, shipborne polarimetric backscatter measurements of Great Lakes (freshwater) ice types using the Jet Propulsion Laboratory C-band scatterometer, together with surface-based ice physical characterization measurements and environmental parameters, were acquired concurrently with Earth Resource Satellite 2 (ERS-2) and RADARSAT Synthetic Aperture Radar (SAR) data (Nghiem and Leshkevich, 1997). This polarimetric data set, composed of over 20 variations of different ice types measured at incident angles from 0° to 60° for all polarizations, was processed to radar cross-section to establish a library of signatures (look-up table) for different ice types. The library is used in the computer classification of calibrated satellite SAR data. Computer analysis of ERS-2 and RADARSAT ScanSAR images of Great Lakes ice cover using a supervised classification technique indicates that different ice types in the ice cover can be identified and mapped (Figure 1), and that wind speed and direction can have an influence on the classification of water as ice based on single frequency, single polarization data (Leshkevich and Nghiem, 1997).

Using RADARSAT-2 Quad-pol and ENVISAT ASAR dual-pol data obtained for Lake Superior during the 2009 and 2011 winter seasons, algorithms were developed for small incidence angle

(<35°) using HH polarization and for large incidence angle (>35°) SAR images using the VV/HH ratio and applied to map ice and open water. Ice types were subsequently classified using the library of backscatter signatures (Leshkevich and Nghiem, 2013). For the small incidence angle data, three of the ice types were combined owing to the overlapping backscatter signatures from these types (lake ice with crusted windrowed snow, rough consolidated ice flows, and stratified ice) in HH polarized data. However, at small incidence angles, these types can be better differentiated in VV polarized data and this needs further investigation for possible algorithm improvement. For HH polarized data at large incidence angles, the various types can be well identified (Figure 2). However, RADARSAT-2 and SENTINEL-1 ScanSAR Wide data are used for the desired synoptic coverage of the Great Lakes, but lack the needed HH and VV polarizations. Other options available to map ice and water are used.

2. MODIS Thermal Infrared Data

NASA's Earth Observing System (EOS) provides space-borne instruments suitable for snow/ice observations. The Terra satellite was launched in December 1999, and the Aqua satellite was launched in May 2002, both having the Moderate Resolution Imaging Spectroradiometer (MODIS) instruments in their payload. A “true-color” MODIS image can be produced using bands 1 (620-670 nm), 4 (545–565 nm) and 3(459–479 nm), such as can be seen in the MODIS Aqua image showing cloud streets over Lake Superior in Figure 3a. A true color image is created by combining Level 1B image data from bands 1, 4 and 3, to create an image with somewhat realistic colors. If desired, the colors can then be “stretched” to enhance our ability to visualize certain features on the Earth.

Moreover, MODIS can measure surface temperature using thermal infrared (TIR) sensors. The present study focuses on TIR surface temperature measurements from the land-surface temperature (LST) (Wan et al., 2002) and ice-surface temperature (IST) (Hall et al., 2004) standard products derived from MODIS data. The MODIS instrument acquires data in 36 spectral channels. MODIS scans $\pm 55^\circ$ from nadir and provides daytime and nighttime imaging of any point on the Earth every 1–2 days. Channels 31 and 32 centered on 11.03 and 12.02 μm , respectively, are used to produce the LST IR surface temperatures that are discussed in this study. MODIS IR radiances have a ground resolution of 1 km at nadir. MODIS IR radiances are calibrated with a cold space view and full aperture black body viewed before and after each Earth view. IST data have been successfully used to identify ice and water in the Arctic (Nghiem et al., 2014), and can be used for the identification of ice versus water across the Great Lakes in a similar manner.

3. Combination of MODIS and SAR Data

Because multi-spectral data and radar data are related to different parameters in the environments, their combination is a good synergy to provide more information to better understand the remote sensing signatures guiding new algorithm development. Here, we show an example of MODIS-observed atmospheric effects, from channels 1, 4, and 3 of MODIS Terra, that impact radar signatures measured by RADARSAT-2 SAR. The results in Figure 3a shows cloud streets oriented primarily in the NW-SE direction extensively over Lake Superior as seen by MODIS on 18 January 2016. The RADARSAT-2 image in Figure 3b on the same date revealed features on the open-water surface across Lake Superior in the same NW-SE direction corresponding to the cloud street pattern in the MODIS image. The observations from the

combination of the contemporaneous MODIS and RADARSAT-2 images show that atmospheric effects due to horizontal convective rolls, creating the cloud streets (von Kármán vortex streets), are responsible for changes over the water surface that impact the radar backscatter signatures.

This demonstrates that backscatter over open water is not only affected by wind speed and wind direction but also modulated by the convective rolls in the planetary boundary layer. Such atmospheric factor needs to be considered in the development of an advanced geophysical model function to improve wind-vector retrieval algorithms. While cloud streets usually occur over the Great Lakes, they are also found over ocean surfaces in the Arctic (Levy 2001, Mourad and Walter 1996, Li et al. 2008) where winds are important to the advance and retreat of sea ice (Nghiem et al. 2006).

3. Dual Polarized Scatterometer Data

Algorithms have also been developed for Great Lakes ice cover mapping using satellite scatterometer data, with large spatial coverage and high temporal resolution, for applications to marine resource management, lake fisheries and ecosystem studies, Great Lakes climatology, and winter navigation. Scatterometer data were acquired over the Great Lakes by NSCAT (NASA Scatterometer) on ADEOS (ADvanced Earth Observing Satellite) in 1996 and 1997, and by the SeaWinds Scatterometer (denoted as QSCAT hereon) operational on the QuikSCAT satellite (1999 - 2009). The follow-on SeaWinds scatterometer launched on the Japanese Midori-II Satellite in December 2002, together with the present scatterometer data sets, can provide long-term decadal data for Great Lakes ice mapping.

The ice-mapping algorithm requires a strict collocation of QSCAT data in time and in space. For each pixel, we form a triplet of collocated and contemporaneous data consisting of forward-look backscatter with vertical polarization (VV_{for}), aft-look backscatter with vertical polarization (VV_{aft}), and forward-look backscatter with horizontal polarization (HH_{for}). Then, these triplets are used in the algorithm development based on the different characteristics between ice and water in radar signatures: (a) large difference in HH_{for} and VV_{for} over water, (b) large variability in VV_{for} and VV_{aft} over water, and (c) surface scattering from water surface can be below the radar noise floor. Figure 4 presents a prototype ice-cover product for the Great Lakes mapped to 12.5 km, which demonstrates that ice extent can be determined and mapped over the Great Lakes with the large-scale coverage of scatterometer data. Another advantage of QSCAT or similar scatterometer data is the capability for daily observations, which allows the monitoring of melting and freezing condition of the Great Lakes ice cover to determine ice freeze-up and break-up dates, of use in climate change studies. Future increases in scatterometer spatial resolution will improve these results.

4. Lake-Wide Light Transmittance Through Ice Using SAR Ice Type Classification Maps

To calculate Great Lakes primary productivity during the approximate four months when the Great Lakes are partially or completely ice covered requires knowledge of the attenuation of light in the PAR region of the electromagnetic spectrum. As reported by Bolsenga et al, (1996) per cent light transmission in the Western Basin of Lake Erie varied from approximately 85% for clear ice to a low of 3% for snow covered ice. Given this large variability in per cent transmission due to ice type and snow cover, an approach to obtain the needed transmission loss values for the primary productivity estimation would be to utilize the NOAA /GLERL produced

ice type maps for the Great Lakes and match an average transmission loss to each major ice type. The snow cover could be factored in using meteorological or satellite observations (Figure 5).

To quantify the effects of ice and snow cover on the Great Lakes on light transmittance, a series of radiometric measurements in the Photosynthetically Active Radiation (PAR) spectral range (400-700nm) were made above the snow/ice interface, at the snow/ice interface, and at the water/ice interface on Lakes Superior and Michigan, as well as a number of smaller inland freshwater lakes during the 2015 and 2016 winter. The PAR irradiance measurements were made using a calibrated Analytical Spectral Device (ASD) ViewSpec 3, Biospherical instruments 4π PAR sensor and a homemade 2π PAR sensor. The majority of the sites sampled were a mixture of snow ice / lake ice, the exception being the Lake Superior sites in L'Anse Bay and a site on Green Bay. In general, the Lake Superior clear ice permitted nearly all light through. The mixed snow ice / lake ice attenuation varied depending on the rheology of the ice, though consistently blocked 50-85% of the PAR. Snow cover of any depth blocked the majority of light and has a well-defined linear relationship from our limited field sampling.

5. GPR Measurements of Ice Thickness

Ice thickness is another characteristic needed for many ecological, modeling, and operational endeavors. In collaboration with the Canadian Coast Guard, a ground penetrating radar (GPR) was tested to retrieve transects of ice thickness from airborne (helicopter) platforms. The GPR (Noggin 1000) is an L-band radar (Figure 6a) that was mounted on a Canadian Coast Guard helicopter (Figure 6b) and flown over Midland Harbor, Ontario in February of 2012. Since the helicopter altitude varies during flight, the ice surface reflector appears to move up and down through the cross-section image. The second reflector, parallel to the ice surface reflector is the bottom of ice. The time difference between these two reflectors indicates the ice thickness. The GPR can be used as a radar altimeter. The helicopter height varied from 6.5 to 10 m up to 23 m along the test transect. Airborne GPR data needs to be compensated for platform elevation. Noggin height above the ground was tabulated and topographic correction was applied resulting in the compensated data. The compensated data show ice thickness was fairly uniform at approximately 29 cm, confirmed by holes augured in the ice along the test transect. The success of these measurements was aided by the smoothness of the ice. With little surface roughness to scatter the GPR signals, maximum signal penetration was achieved. The next step is to use autonomous drones, for which initial drone tests were successfully carried out across cold snow and ice environment under various wind conditions in March 2016. Additional tests need to be conducted to determine measurement accuracy over other ice types, and whether the GPR can be successfully flown on an autonomous drone, which can also be used to carry a sonar and infrared sensors to obtain snow/ice thickness and surface temperature.

Acknowledgments

GLERL Contribution No. xxx. The research at the Jet Propulsion Laboratory, California Institute of Technology, was supported by NASA and NOAA.

References

Bolsenga SJ, Evans M, Vanderploeg HA, Norton DG. 1996. PAR transmittance through thick, clear freshwater ice. *Hydrobiologia* 330: 227–230. <http://dx.doi.org/10.1007/BF00024210>

- Bryan, M.L. 1975. *A comparison of ERTS-1 and SLAR data for the study of surface water resources*. Final Report, ERIM No. 193300-59-F, prepared for the National Aeronautics and Space Administration by the Environmental Research Institute of Michigan, Ann Arbor, MI under Contract No. NAS5-21783.
- Chase, P.E. 1972. *Guide to ice interpretation: Satellite imagery and drift ice*. Final Report prepared for the U.S. Department of Commerce by The Bendix Corp, Aerospace Systems Division, Ann Arbor, MI, under Contract No. 2-35372.
- Hall, D. K., Key, J., Casey, K.A., Riggs, G.A. and Cavalieri, D.J., 2004. Sea ice surface temperature product from MODIS. *IEEE Trans. Geosci. Remote Sens.*, 42:1076–1087.
- Lalumiere, L. 2006 “Ground Penetrating Radar for Helicopter Snow and Ice Surveys”. *Can. Tech. Rep. Hydrogr. Ocean Sci.* 248: iv+44 p.
- Leshkevich, G.A. 1976. Great Lakes ice cover, winter 1974–75, NOAA Technical Report ERL 370-GLERL 11. National Technical Information Service, Springfield, VA 22161, 42 pp.
- Leshkevich, G.A., Nghiem, S.V., 2007. Satellite SAR remote sensing of Great lakes ice cover, part 2. Ice classification and mapping. *J. Great Lakes Res.* 33 (4), 736–750.
- Leshkevich, G. and S.V. Nghiem. 2013. Great Lakes ice classification using satellite C-band SAR multi-polarization data. *Journal of Great Lakes Research Supplement* 39: 55–64.
- Levy, G. 2001. Boundary layer roll statistics from SAR. *Geophysical Research Letters*, 28(10): 1993–1995.
- Li, X., Zheng, W., Zou, C.-Z., Pichel, W. 2008. A SAR Observation and Numerical Study on Ocean Surface Imprints of Atmospheric Vortex Streets. *Sensors*, 8, 3321–3334; doi: 10.3390/s8053321.
- Marshall, E.W. 1966. *Air photo interpretation of Great Lakes ice features*. Great Lakes Research Division, Special Report No. 25, University of Michigan, Ann Arbor, MI.
- McGinnis, D.F., and Schneider, S.R. 1978. Monitoring river ice breakup from space, *Photogrammetric Engineering & Remote Sensing* 44(1):57–68.
- McMillan, M.C., and Forsyth, D.G. 1976. *Satellite images of Lake Erie ice, January–March 1975*, NOAA Technical Memorandum NESS-80, National Technical Information Service, Springfield, VA 22161.
- Mourad, P.D., and Walter, B.A. 1996. Viewing a cold air outbreak using satellite-based synthetic aperture radar and advanced very high resolution radiometry imagery. *Journal of Geophysical Research*, 101(C7): 16,391–16,400.

- Nghiem, S.V., Hall, D.K., Rigor, I.G., Li, P., and Neumann, G. 2014. Effects of Mackenzie River discharge and bathymetry on sea ice in the Beaufort Sea. *Geophys. Res. Lett.*, 41(3), doi:10.1002/2013GL058956.
- Nghiem, S.V., and Leshkevich, G.A., 2007. Satellite SAR remote sensing of Great Lakes ice cover, part 1. Ice backscatter signatures at C-band. *J. Great Lakes Res.* 33 (4), 722–735.
- Nghiem, S.V., Chao, Y., Neumann, G., Li, P., Perovich, D.K., Street, T., and Clemente-Colón, P. (2006). Depletion of perennial sea ice in the East Arctic Ocean, *Geophysical Research Letters*, 33, L17501, doi:10.1029/2006GL027198.
- Nghiem, S.V., and Leshkevich, G.A., 2003. Great Lakes Ice Mapping with Satellite Scatterometer Data. Report JPL D-26362, Jet Propulsion Laboratory, 27 pg.
- Rondy, D.R. 1971. *Great Lakes ice atlas*. NOAA Technical Memorandum NOS LSCR 1, National Technical Information Service, Springfield, VA, 22161.
- Rumer, R.R., Crissman, R., and Wake, A. 1979. *Ice transport in Great Lakes*. Water Resources and Environmental Engineering Research Report No. 79-3 prepared for the Great Lakes Environmental Research Laboratory by the State University of New York at Buffalo, Department of Civil Engineering, and the Center for Cold Regions Engineering, Science and Technology, under Contract No. 03-78-B01-104.
- Schertler, R.J., Mueller, R.A., Jirberg, R.J., Cooper, D.W., Heighway, J.E., Homes, A.D., Gedney, R.T., and Mark, H. 1975. *Great Lakes all-weather ice information system*, NASA Technical Memorandum NASA TM X-71815, National Technical Information Service, Springfield, VA, 22161.
- Schneider, S.R., McGinnis, D.F., Jr., and Gatlin, J.A. 1981. *Use of NOAA/AVHRR visible and near-infrared data for land remote sensing*. NOAA Technical Report NESS-84, National Technical Information Service, Springfield, VA 22161.
- Strong, A.E. 1973. New sensor on NOAA-2 satellite monitors during the 1972–73 Great Lakes ice season. In *Remote Sensing and Water Resources Management. Proceedings No. 17*, pp. 171–178. American Water Resources Association, Urbana, IL.
- Wan, Z., 2008. New refinements and validation of the MODIS and-surface temperature/emissivity products. *Remote Environ.*, 112, 59–74, doi:10.1016/j.rse.2006.06.026.
- Wartha, J.H., 1977. Lake Erie Ice—Winter 1975–76. NOAA Technical Memorandum

Figures

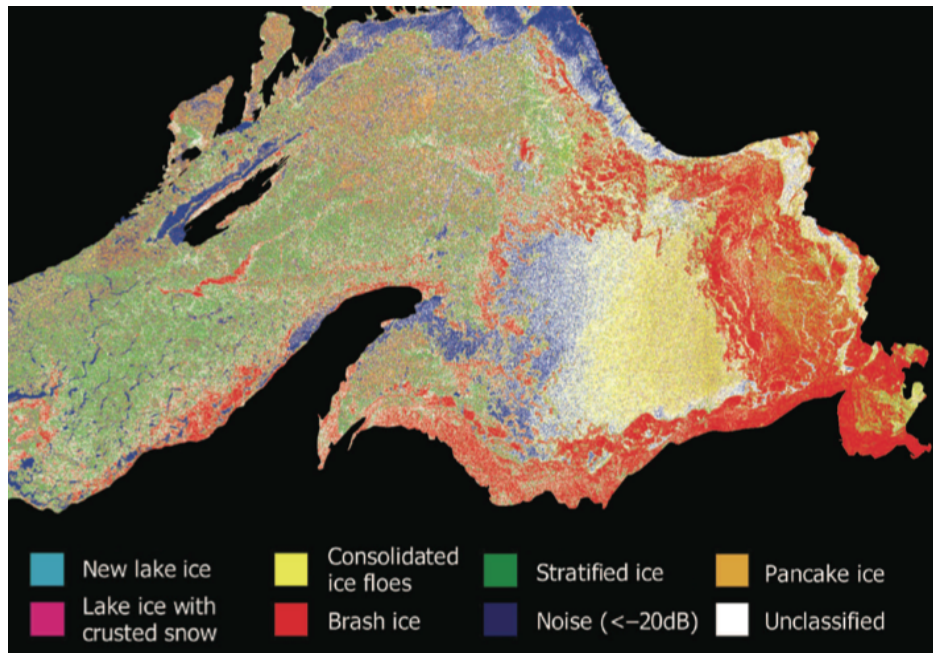


Figure 1. Classified color-coded RADARSAT-1 scene (22 March 1997) calibrated to σ_0 by Satlantic, Inc. Measured backscatter values were used as training sets. Areas below the RADARSAT noise floor (-20 dB) are coded blue and unclassified areas are coded white.

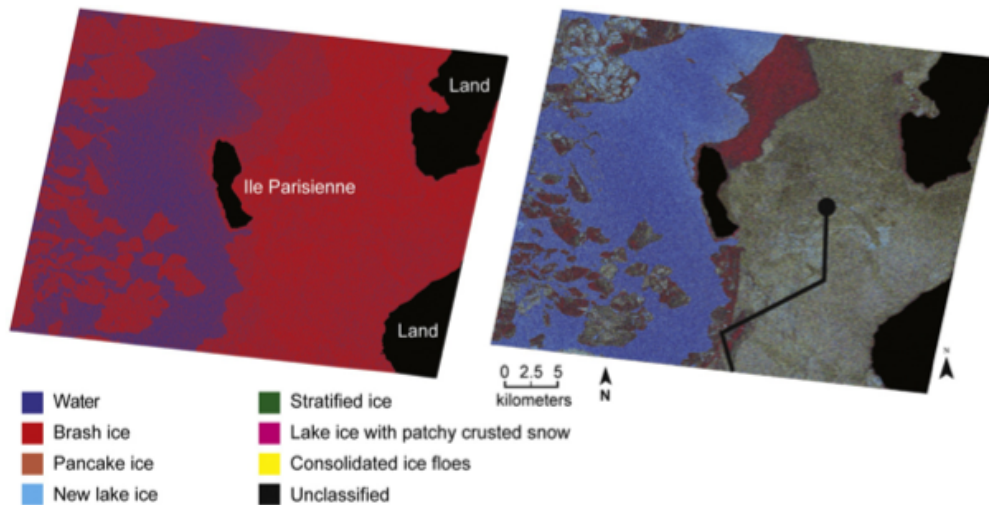


Figure 2. Results for ice and open water identification (left panel) using the co-polarization ratio $r = VV / HH$ from the RADARSAT-2 SAR scene at large incidence angles collected on March 20, 2011 over Whitefish Bay in Lake Superior. Red is for ice and blue for open water. The right panel shows the results of the ice signature library applied to the HH scene for ice classification once water is identified. The black line is the approximate the USCGC Mackinaw ship track in the ice east of Ile Parisienne on 24 March 2011 where “ground truth” data were collected.

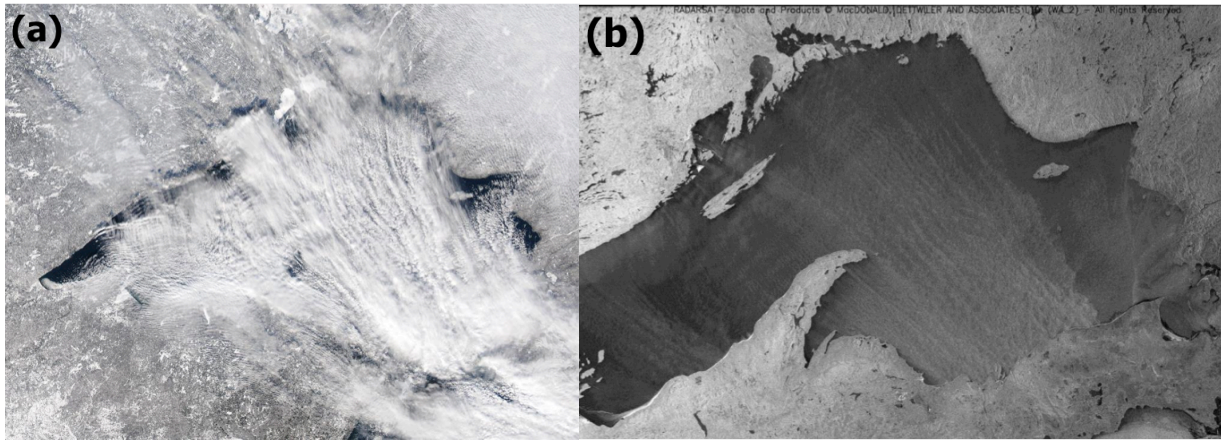


Figure 3. Cloud streets observed by MODIS on 18 January 2016 in the top panel (a), and effects on RADARSAT-2 SAR backscatter pattern on the same day in the bottom panel (b).

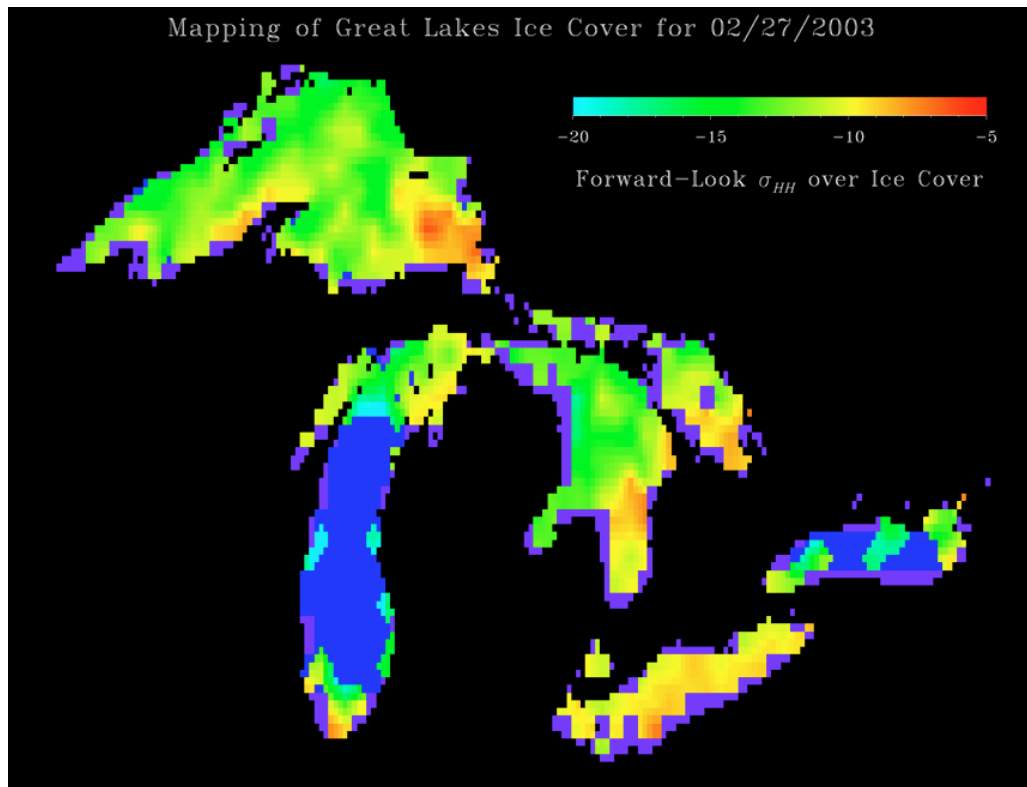


Figure 4. Prototype of ice-cover product for the Great Lakes mapped to 12.5 km: green-red for ice, blue for water, and violet for unclassified areas.

Measuring Light Transmittance Through Ice Cover

Light Attenuation Through Snow Ice on Lake Ice With and Without a Snow cover



Lake Superior ice type classification - March 20, 2014 using RADARSAT-2 SAR image. Ice type maps for the Great Lakes can be matched with average transmission loss for each generic ice type. The snow cover could be factored in using meteorological or satellite observations.

Figure 5. Satellite synthetic aperture radar (SAR) ice type classification maps can be used together with average PAR transmission for major ice types to create estimates of lake-wide PAR transmission.

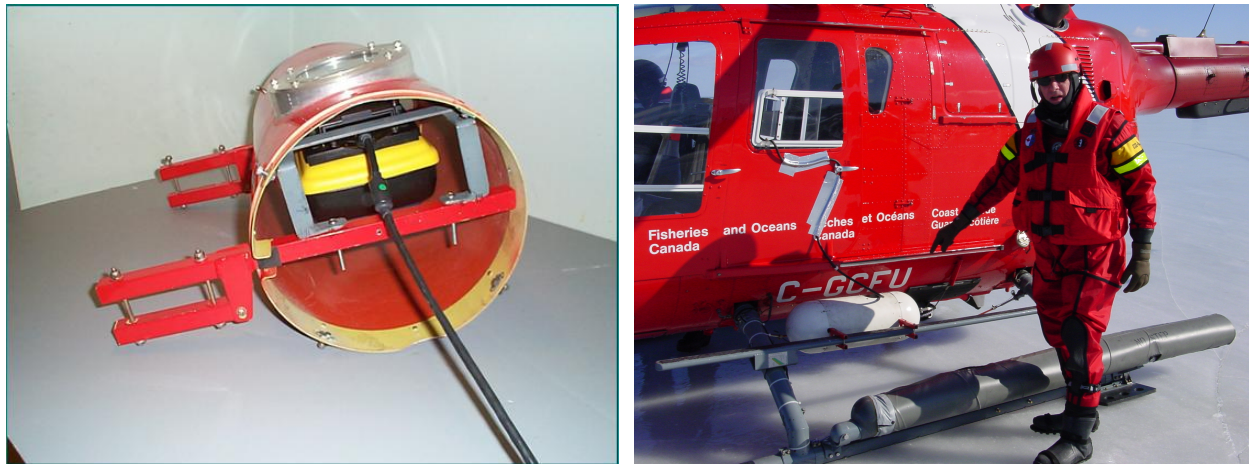


Figure 6. (a) Left panel for NOGGIN ground penetrating radar (GPR) in environmental case, and (b) right panel for GPR in environmental case mounted on Canadian Coast Guard helicopter.